THE JOURNAL OF BIOLOGICAL CHEMISTRY VOL. 284, NO. 39, pp. 26533–26546, September 25, 2009

Hyaluronan-CD44 Interaction with Protein Kinase Cϵ Promotes Oncogenic Signaling by the Stem Cell Marker Nanog and the Production of MicroRNA-21, Leading to Down-regulation of the Tumor Suppressor Protein PDCD4, Anti-apoptosis, and Chemotherapy Resistance in Breast Tumor Cells*

Received for publication, May 29, 2009, and in revised form, July 16, 2009 Published, JBC Papers in Press, July 24, 2009, DOI 10.1074/jbc.M109.027466

Lilly Y. W. Bourguignon[1], **Christina C. Spevak, Gabriel Wong, Weiliang Xia, and Eli Gilad**

From the Endocrine Unit, Department of Medicine, University of California at San Francisco, and Veterans Affairs Medical Center, San Francisco, California 94121

Multidrug resistance and disease relapse is a challenging clinical problem in the treatment of breast cancer. In this study, we investigated the hyaluronan (HA)-induced interaction between CD44 (a primary HA receptor) and protein kinase Cϵ (PKCϵ), which regulates a number of human breast tumor cell functions. Our results indicate that HA binding to CD44 promotes PKCϵ activation, which, in turn, increases the phosphorylation of the stem cell marker, Nanog, in the breast tumor cell line MCF-7. Phosphorylated Nanog is then translocated from the cytosol to the nucleus and becomes associated with RNase III DROSHA and the RNA helicase p68. This process leads to microRNA-21 (miR-21) production and a tumor suppressor protein (*e.g.* PDCD4 (program cell death 4)) reduction. All of these events contribute to up-regulation of inhibitors of apoptosis proteins (IAPs) and MDR1 (multidrug-resistant protein), resulting in anti-apoptosis and chemotherapy resistance. Transfection of MCF-7 cells with PKCϵ or Nanog-specific small interfering RNAs effectively blocks HA-mediated PKCϵ-Nanog signaling events, abrogates miR-21 production, and increases PDCD4 expression/eIF4A binding. Subsequently, this PKCϵ-Nanog signaling inhibition causes IAP/MDR1 down-regulation, apoptosis, and chemosensitivity. To further evaluate the role of miR-21 in oncogenesis and chemoresistance, MCF-7 cells were also transfected with a specific anti-miR-21 inhibitor in order to silence miR-21 expression and inhibit its target functions. Our results indicate that anti-miR-21 inhibitor not only enhances PDCD4 expression/eIF4A binding but also blocks HA-CD44-mediated tumor cell behaviors. Thus, this newly discovered HA-CD44 signaling pathway should provide important drug targets for sensitizing tumor cell apoptosis and overcoming chemotherapy resistance in breast cancer cells.

Chemotherapeutic failure frequently contributes to morbidity in patients diagnosed with solid tumors, such as breast cancers (1–3). Recent studies indicate that oncogenic signaling and tumor cell-specific function are directly involved in chemotherapeutic drug resistance and breast tumor progression (4–6). A number of studies have aimed at identifying those molecules that are specifically expressed by epithelial tumor cells and correlate with metastatic behavior and chemoresistance. Among such molecules is hyaluronan (HA),[2] a major component in the extracellular matrix of most mammalian tissues (7, 8). HA is a nonsulfated, unbranched glycosaminoglycan, consisting of repeating disaccharide units, D-glucuronic acid, and *N*-acetyl-D-glucosamine (9, 10). The biosynthesis of HA is regulated by three mammalian HA synthase isozymes, HA synthase 1, 2, and 3 (11–14). Abnormal production of HA directly contributes to aberrant cellular processes, such as transformation and metastasis (15). Furthermore, HA is digested into a variety of smaller-sized molecules by various hyaluronidases (16). Activation of extracellular matrix-degrading enzymes, such as the hyaluronidases, appears to be closely associated with tumor progression (17). In addition, HA is enriched in many types of tumors (18, 19). In particular, HA levels are found to be elevated in the serum of breast cancer patients (20). In certain tumor types, the level of HA has been found to be predictive of malignancy (19).

HA binds specifically to CD44, a family of multifunctional transmembrane glycoproteins expressed in numerous cells and tissues, including breast tumor cells and various carcinoma tissues (4, 8, 21–24). CD44 is generally expressed in a variety of isoforms that are products of a single gene generated by alternative splicing of variant exons inserted into an extracellular membrane-proximal site (25, 26). CD44 is also expressed in tumor stem cells that have the unique ability to initiate tumor cell-specific properties (27). In fact, CD44 is proposed to be one

* This work was supported, in whole or in part, by National Institutes of Health Grants R01 CA66163, R01 CA 78633, and P01 AR39448. This work was also supported by a Veterans Affairs Merit Review grant and a Department of Defense grant.

[1] A Veterans Affairs Senior Research Career Scientist. To whom correspondence should be addressed: Endocrine Unit (111N), Dept. of Medicine, University of California at San Francisco, and Veterans Affairs Medical Center, 4150 Clement St., San Francisco, CA 94121. Tel.: 415-221-4810 (ext. 3321); Fax: 415-383-1638; E-mail: lilly.bourguignon@ucsf.edu.

[2] The abbreviations used are: HA, hyaluronan; TGFβ, transforming growth factor β; PKC, protein kinase C; IAP, inhibitor of apoptosis protein; MDR, multidrug-resistant; miRNA, microRNA; miR-21, microRNA-21; CHAPS, 3-[(3-cholamidopropyl)dimethylammonio]-1-propanesulfonic acid; FITC, fluorescein isothiocyanate; XIAP, X-linked IAP.

of the important surface markers on cancer stem cells (27). HA binding to CD44 is known to be involved in the stimulation of both receptor kinases (*e.g.* ErbB2, epidermal growth factor receptor, and TGFβ receptors) and non-receptor kinases (*e.g.* c-Src and ROK) (28–34) required for a variety of tumor cell-specific functions leading to tumor progression.

Protein kinase C (PKC), a family of serine-threonine kinases, plays a pivotal role in signal transduction and a number of cellular functions (35). It consists of at least 11 different isoforms, including the novel type of PKC isoforms, such as PKCε (36). A previous study found that PKCε is associated with the anti-apoptotic Bcl-2 family of proteins (37). PKC also functions to prevent apoptosis in a number of cells by up-regulating inhibitors of apoptosis (IAP) proteins (*e.g.* X-linked IAP (XIAP) and survivin) and by inhibiting caspases (37, 38). Down-regulation of PKCε by treating cells with PKC inhibitors sensitizes tumor necrosis factor-α-mediated cell death in breast tumor cells (39). Thus, PKCε appears to be functionally linked to anti-apoptotic effects and survival pathways in tumor cells.

In addition, activation of certain PKC isoforms has been implicated in the induction and maintenance of the multidrug-resistant (MDR) phenotype (40). Specifically, an increase in PKCε expression is closely associated with the drug-resistant phenotype in epithelial tumor cells (40). P-glycoprotein (P-gp), the product of the *MDR1* (*ABCB1*) gene, is a transmembrane ATP-dependent transporter known to play a role in drug fluxes and chemotherapeutic resistance in a variety of cancers (41). A number of studies have shown that both HA and CD44 are involved in chemotherapeutic drug resistance in many cancer types (5, 6, 42–48). In particular, the stem cell marker, Nanog, appears to interact with Stat-3 (signal transducer and activator of transcription protein 3) in the nucleus, leading to transcriptional activation, *MDR1*/*P-gp* expression, and chemotherapy resistance in HA-CD44-activated breast tumor cells (5). The question of whether there is a functional link between PKCε and Nanog signaling in HA-CD44-mediated oncogenesis and drug resistance in breast tumor cells has not yet been addressed.

The miRNAs are evolutionarily conserved and function as negative regulators of gene expression by inhibiting the expression of mRNAs that contain complementary target sites referred to as the "seed region" (49). Previous data have revealed that human miRNAs are processed from capped and polyadenylated transcripts that are precursors to the mature miRNAs (pri-miRNAs) (50). In mammalian miRNA biogenesis, primary transcripts of miRNA genes (pri-mRNAs) are subsequently cleaved to produce an intermediate molecule containing a stem loop of ~70 nucleotides (pre-mRNAs) by the nuclear RNase III enzyme DROSHA and exported from the nucleus by exportin 5 (49). A second RNase III enzyme, Dicer, then generates the mature miRNA, which is loaded into the RNA-induced silencing complex in association with the argonaute protein that induces silencing via the RNA interference pathway (51). Although Dicer has an important role in the silencing action of miRNAs, recent studies have shown that silencing can still occur in cells that lack Dicer (52). It has recently been shown that the nuclear p68-RNA helicase is required in the uptake of certain miRNAs into the silencing complex (53). p68 belongs to a family of proteins that are involved in RNA metabolism processes, such as translation and RNA degradation (54). A previous study showed that miR-21 processing or biogenesis (via the precursor pri-miR-21) required p68 and DROSHA in breast tumor cells (55). Several transcription factors, including Nanog, also appear to be involved in the regulation of pri-miRNA expression during development (56). Whether HA-CD44-mediated signaling is involved in miR-21 maturation/production and chemotherapy resistance in breast tumor cells has not been determined.

Accumulating evidence indicates the involvement of non-coding miRNAs (~22 nucleotides) in both cancer development and multidrug resistance (57). Analysis of the array profile of miRNA expression in normal breast and breast carcinoma tissues reveals that miRNA-21 (miR-21) is abundantly produced in tumors compared with normal tissues (57). The functional significance of miR-21 has been elucidated in several recent studies following the discovery of its specific targets (58). miR-21 is now one of the most studied miRNAs due to its involvement in cancer progression. It has recently been shown that miR-21 plays a role in the inhibition of a tumor suppressor protein, such as PDCD4 (program cell death 4) via a conserved site within the 3′-untranslated region of the mRNA (58, 82). Down-regulation of PDCD4 expression by miR-21 leads to tissue invasion and metastasis (58, 82). Thus, miR-21 is currently considered to be an oncogene.

In this study, we have investigated a novel HA-CD44-mediated PKCε signaling mechanism that regulates the stem cell marker (Nanog)-associated miR-21 production. Our results indicate that HA-CD44-activated PKCε stimulates Nanog phosphorylation, which in turn, activates Nanog signaling-regulated miR-21 production. These events lead to the tumor suppressor protein (PDCD4) reduction, IAP/MDR1 (P-gp) overexpression, anti-apoptosis, and chemoresistance in breast tumor cells. Inhibition of either PKCε-Nanog signaling or silencing of miR-21 expression/function by transfecting breast tumor cells with PKCε siRNA (or Nanog siRNA) or anti-miR-21 inhibitor not only results in PDCD4 up-regulation and PDCD4-eIF4A complex formation but also causes a reduction of IAP/MDR1 (P-gp) and an enhancement of apoptosis and chemosensitivity. Our findings provide important new insights into understanding the roles that HA-CD44-mediated PKCε activation and Nanog-regulated miR-21 play in regulating anti-apoptosis and chemotherapy resistance in breast tumor cells.

MATERIALS AND METHODS

Cell Culture—Human breast tumor cell line MCF-7 cells were purchased from ATCC (Manassas, VA) and grown in RPMI 1640 medium supplemented with 10% fetal bovine serum. Cells were routinely serum-starved (and thereby deprived of serum HA) before adding HA.

Antibodies and Reagents—Monoclonal rat anti-CD44 antibody (clone 020; isotype IgG_{2b}; obtained from CMB-TECH, Inc., San Francisco, CA) recognizes a determinant of the HA-binding region common to CD44 and its principal variant isoforms (21–24, 28–34). This rat anti-CD44 was routinely used for HA-related blocking experiments and immunoprecipitation. Immunoreagents, such as rabbit anti-PKCε antibody, goat anti-Nanog antibody, mouse anti-PDCD4 antibody, rabbit

anti-MDR1 (P-glycoprotein 170) antibody, and goat anti-actin antibody were purchased from Santa Cruz Biotechnology, Inc. (Santa Cruz, CA). Several immunoreagents, including rabbit anti-DROSHA antibody, mouse anti-p68 antibody, and rabbit anti-phosphoserine antibody, were obtained from Millipore (Billerica, MA). Rabbit anti-eIF4A and rabbit anti-survivin were purchased from Cell Signaling Technology, Inc. (Danvers, MA) and Abcam (Cambridge, MA), respectively. Mouse anti-XIAP antibody was from BD Biosciences. Doxorubicin hydrochloride and paclitaxel (Taxol) were obtained from Sigma. Healon HA polymers (~500,000-dalton polymers), purchased from Amersham Biosciences and The Upjohn Co. were prepared by gel filtration column chromatography, using a Sephacryl S1000 column. The purity of the HA polymers used in our experiments was further verified by anion exchange high performance liquid chromatography, followed by protein and endotoxin analyses, using the BCA protein assay kit (Pierce) and an *in vitro* limulus amebocyte lysate assay (Cambrex Bio Science, Inc., Walkersville, MD), respectively. No protein or endotoxin contamination was detected in this HA preparation. PKCϵ substrate peptide-2 was obtained from Millipore (Billerica, MA).

PKCϵ siRNA-Nanog siRNA Preparations and Transfection—The siRNA sequence targeting human PKCϵ and Nanog (from mRNA sequence; GenBank™ accession number NM_005400 and NM_024865, respectively) corresponds to the coding region relative to the first nucleotide of the start codon. Target sequences were selected, using the software developed by Ambion Inc. As recommended by Ambion, PKCϵ- or Nanog-specific targeted regions were selected beginning 50–100 nucleotides downstream from the start codon. Sequences close to 50% G/C content were chosen. Specifically, PKCϵ siRNA, PKCϵ-specific target sequence (AAGATGAAGGAGGCGCTCAGTT), and scrambled sequences were used. In the case of Nanog, Nanog-specific target sequences (target 1, AATCTTCACCTATGCCTGTGA; target 2, AATGAAATCTAAGAGGTGGA; target 3, AAACCATGGATTTATTCCTAA) and scrambled sequences were used. MCF-7 cells were then transfected with siRNA, using siPORT Lipid as transfection reagent (Silencer™ siRNA transfection kit; Ambion) according to the protocol provided by Ambion. Cells were incubated with 50 pmol of PKCϵ siRNA or Nanog siRNA or 50 pmol of siRNA containing scrambled sequences or no siRNA for at least 24 h before biochemical experiments.

Anti-miR-21 Inhibitor Preparation and Transfection—Anti-miR™ targeting miR-21 (anti-miR-21 inhibitor) (catalogue number 17000; Ambion) and its corresponding negative control (catalogue number 17010; Ambion) were transfected into MCF7 cells, using Lipofectamine 2000 reagent (Invitrogen) for 24 h. Cells were then treated with HA or without HA in various experiments, as described below. The final concentrations of anti-miR-21 and miRNA-negative control used in various experiments were 30 nmol/liter.

Preparations of Cell Lysate, Cytoplasm, and Nucleus Fractions—MCF-7 cells (untreated or treated with PKCϵ siRNA or Nanog siRNA or siRNA with scrambled sequences or pretreated with anti-CD44 antibody) were incubated with HA (50 μg/ml) (or without HA) for various time intervals (*e.g.* 0 min, 5 min, 10 min, 15 min, 30 min, or 24 h) at 37 °C. Cells were then lysed in a lysis buffer (50 mM HEPES (pH 7.5), 150 mM NaCl, 20 mM $MgCl_2$, 0.5% Nonidet P-40 (Nonidet P-40), 0.2 mM Na_3VO_4, 0.2 mM phenylmethylsulfonyl fluoride, 10 μg/ml leupeptin, and 5 μg/ml aprotinin). Both cytoplasmic and nuclear fractions were prepared, using the extraction kit from Active Motif (Carlsbad, CA) according to the protocols provided by the manufacturer.

Immunoprecipitation and Immunoblotting Techniques—Both cell lysate and the cytosolic fraction of MCF-7 cells (pretreated with anti-CD44 antibody or transfected with PKCϵ siRNA, Nanog siRNA, siRNA with scrambled sequences, anti-miR-21 inhibitor, or miRNA-negative control or without any treatment, followed by HA (50 μg/ml) addition (or no HA addition) for various time intervals (*e.g.* 0 min, 5 min, 10 min, 15 min, 30 min, or 24 h) at 37 °C) were immunoblotted using various immunoreagents (*e.g.* rabbit anti-PKCϵ (2 μg/ml), goat anti-Nanog (2 μg/ml), rabbit anti-MDR1 (2 μg/ml), mouse anti-PDCD4 (2 μg/ml), rabbit anti-eIF4A (2 μg/ml), rabbit anti-survivin (2 μg/ml), mouse anti-XIAP, or goat anti-actin (2 μg/ml) (as a loading control), respectively).

In addition, immunoprecipitation was conducted after homogenization of the cell lysate using rat anti-CD44 antibody, followed by goat anti-rat IgG-beads. Subsequently, the immunoprecipitated materials were solubilized in SDS sample buffer, electrophoresed, and blotted onto nitrocellulose. After blocking nonspecific sites with 3% bovine serum albumin, the nitrocellulose filters were incubated with rabbit anti-PKCϵ antibody (2 μg/ml) for 1 h at room temperature. In some cases, the cell lysates were immunoprecipitated with goat anti-Nanog antibody, followed by rabbit anti-goat IgG-beads. Subsequently, the immunoprecipitated materials were processed for immunoblotting using rabbit anti-phosphoserine antibody (2 μg/ml).

In some cases, the nuclear fraction of MCF-7 cells (untransfected or transfected with PKCϵ siRNA, Nanog siRNA, or scrambled sequence siRNA plus 50 μg/ml HA (or no HA) for various time intervals (*e.g.* 0, 5, 15, or 30 min) at 37 °C was used for rabbit anti-DROSHA antibody-conjugated immunoprecipitation, followed by goat anti-Nanog, mouse anti-p68, or rabbit anti-DROSHA-mediated immunoblot, respectively.

In addition, cell lysates of MCF-7 cells transfected with PKCϵ siRNA (or Nanog siRNA or siRNA with scrambled sequences or anti-miR-21 or miRNA-negative control) were treated with no HA or with HA (50 μg/ml) for 24 h at 37 °C. These lysate samples were then immunoblotted with various immunoreagents (*e.g.* rabbit anti-MDR1 (2 μg/ml), mouse anti-PDCD4 (2 μg/ml), rabbit anti-eIF4A (2 μg/ml), rabbit anti-survivin (2 μg/ml), mouse anti-XIAP, or goat anti-actin (2 μg/ml) (as a loading control), respectively).

Northern Blot Analysis—Total RNA was isolated from MCF-7 cells (untreated or pretreated with anti-CD44 antibody or transfected with PKCϵ siRNA or Nanog siRNA or siRNA with scrambled sequences or anti-miR-21 inhibitor or miRNA-negative control) in the absence or presence of HA for various time intervals (*e.g.* 0 min, 15 min, 30 min, or 2 h) at 37 °C using TriPure Isolation Reagent (Roche Applied Science). The probes were generated using the *mirVana* miRNA probe construction

kit (Ambion), following the manufacturer's instructions. RNA concentrations were verified by measuring absorbance (A_{260}) on the NanoDrop Spectrophotometer ND-1000 (NanoDrop). Total RNA samples (10 μg each) and enriched small RNAs (1 μg) were electrophoresed on 12% acrylamide, 8 M urea gels, stained with ethidium bromide, and transferred using a capillary blotting method overnight onto Hybond-N^+ membrane (Amersham Biosciences). 5 S rRNA was used as a loading control. RNA was immobilized by using a UV transilluminator for 10 min. Prehybridization and hybridization were performed at 40 °C using the ULTRAHyb buffer from the NorthernMax kit (Ambion) for 30 min. Small RNAs were detected using [α-^{32}P]UTP (800 Ci/mmol, 10 mCi/ml), which was used in the transcription reactions to synthesize labeled antisense RNA probe. Radioactively labeled probe was added to the ULTRAHyb buffer at 40 °C for 16 h. Membranes were washed twice for 5 min at room temperature with Low Stringency Washing Solution (equivalent to 2× SSC, 0.1% SDS) and one more time at a hybridization temperature of 40 °C from the NorthernMax kit (Ambion). Sealed blots were exposed to film overnight and visualized using autoradiography.

RNase Protection Assay Analysis of Mature miRNAs—Expression of miRNAs was also qualitatively analyzed by an RNase protection assay. For the RNase protection assay, enriched small RNA isolated from MCF-7 cells (untreated or pretreated with anti-CD44 antibody or transfected with PKCε siRNA, Nanog siRNA, siRNA with scrambled sequences, anti-miR-21 inhibitor, or miRNA-negative control in the presence or absence of HA for various time intervals (*e.g.* 0 min, 5 min, 10 min, 15 min, 30 min, or 2h) at 37 °C) was enriched and purified using the *mirVana* miRNA isolation kit (Ambion). RNA concentrations were verified by measuring absorbance (A_{260}) on the NanoDrop Spectrophotometer ND-1000 (NanoDrop). The *mirVana* miRNA probe construction kit (Ambion) was used to synthesize the ^{32}P-labeled miR-21 antisense probe and miR-191 (60) probe loading control. Probes used were gel-purified using a 12% acrylamide, 8 M urea gel prior to hybridization experiments. Probe hybridization and RNase protection were then carried out using the *mirVana* miRNA detection kit (Ambion) according to the manufacturer's instructions. After hybridization and RNase treatment, the double-stranded product was resolved in a 12% polyacrylamide, 8 M urea denaturing gel and visualized using autoradiography. All samples were treated under similar conditions, and an additional radioactive-labeled probe, miR-191, was used as a loading control.

PKCε-mediated Protein Phosphorylation in Cell-free System—PKCε was prepared by anti-PKCε-conjugated immunoaffinity column chromatography. The PKCε kinase reaction was then performed in 50 μl of the kinase buffer, containing 25 mM Tris-HCl (pH 7.5), 5 mM β-glycerolphosphate, 2 mM dithiothreitol, 0.1 mM Na_3VO_4, 10 mM $MgCl_2$, 0.1% CHAPS, 0.1 μM calyculin A, 200 μM [^{32}P]ATP, 100 ng of PKCε isolated from MCF-7 cells (pretreated with anti-CD44 antibody or transfected with PKCε siRNA or siRNA with scrambled sequences or without any treatment, followed by HA (50 μg/ml) addition (or no HA addition) for various time intervals (*e.g.* 0, 5, 15, or 30 min) at 37 °C), and 1 μg of PKCε substrate peptide-2 or 1 μg of Nanog (obtained from anti-Nanog affinity column). After incubation for 30 min, at 30 °C, the reactions were terminated by adding 20% cold trichloroacetic acid, and 2 mg/ml bovine serum albumin was then added as a carrier. Trichloroacetic acid-precipitated proteins were spotted on 3M filter papers followed by an extensive wash with 10% trichloroacetic acid. The radioactivity associated with trichloroacetic acid-precipitated materials was analyzed by liquid scintillation counting.

Immunofluorescence Staining—MCF-7 cells (transfected with PKCε siRNA or siRNA with scrambled sequences) were incubated with HA (50 μg/ml) at 37 °C for various time intervals (*e.g.* 0, 10, 30, or 60 min) or with no HA). These cells were then fixed with 2% paraformaldehyde. Subsequently, these cells were rendered permeable by ethanol treatment, followed by incubating with fluorescein (FITC)-conjugated anti-Nanog antibody, followed by a monomeric cyanine nucleic acid staining, Topro-3 (a marker for nucleus). To detect nonspecific antibody binding, Topro-3-labeled cells were incubated with FITC-conjugated normal IgG, respectively. No labeling was observed in control samples. These fluorescence-labeled samples were then examined with a confocal laser-scanning microscope.

Tumor Cell Growth Assays—MCF-7 cells were either untreated or pretreated with anti-CD44 antibody or transfected with PKCε siRNA (or Nanog siRNA, siRNA with scrambled sequences, anti-miR-21, or miRNA-negative control) in the presence or absence of HA, as above. These cells were then plated in 96-well culture plates in 0.2 ml of Dulbecco's modified Eagle's medium/F-12 medium supplement (Invitrogen) containing no serum for 24 h at 37 °C in 5% CO_2, 95% air. In each experiment, a total of five plates (6 wells/treatment (*e.g.* HA treatment/plate)) were used. Experiments were repeated 5–6 times. The *in vitro* growth of these cells was determined by measuring increases in cell number using the 3-(4,5-dimethylthiazol-2-yl)-2,5-diphenyltetrazolium bromide assay (CellTiter 96® non-radioactive cell proliferation assay) according to the procedures provided by Promega. Subsequently, viable cell-mediated reaction products were recorded by a Molecular Devices (Spectra Max 250) enzyme-linked immunosorbent assay reader at a wavelength of 450 nm.

In some experiments, MCF-7 cells were pretreated with anti-CD44 antibody or transfected with PKCε siRNA (or Nanog siRNA, siRNA with scrambled sequences, anti-miR-21 inhibitor, or miRNA-negative control or without any treatment), as above. These cells (5×10^3 cells/well) were then incubated with various concentrations of doxorubicin (4×10^{-9} M to 1.75×10^{-5} M) or paclitaxel (3.2×10^{-9} to $\mathrm{M}^{-1} \times 10^{-5}$ M) with no HA or with HA (50 μg/ml). After a 24-h incubation at 37 °C, 3-(4,5-dimethylthiazol-2-yl)-2,5-diphenyltetrazolium bromide-based growth assays were analyzed as described above. The percentage of absorbance relative to untreated controls (*i.e.* cells treated with neither HA nor chemotherapeutic drugs) was plotted as a linear function of drug concentration. The 50% inhibitory concentration (IC_{50}) was identified as a concentration of drug required to achieve a 50% growth inhibition relative to untreated controls.

RESULTS

HA-CD44-mediated PKCε Activation and Nanog Phosphorylation/Signaling in MCF-7 Breast Tumor Cells

PKC belongs to a family of isoforms that are involved in a variety of biological activities (35). Previous studies showed that CD44 and PKC are structurally and functionally coupled in a number of cell types (61–64). As part of our continued effort to investigate CD44-linked PKC activation that correlates with metastatic behaviors, a specific PKC isoform, namely PKCε, was identified. In these studies, we performed anti-CD44-mediated immunoprecipitation, followed by anti-PKCε immunoblot (Fig. 1*A*, *a*, *lane 1*) or anti-CD44 immunoblot (Fig. 1*A*, *b*, *lane 1*), using untreated MCF-7 cells. Our results indicate that a very low level of PKCε (Fig. 1*A*, *a*, *lane 1*) is present in the anti-CD44-immunoprecipitated materials (Fig. 1*A*, *b*, *lane 1*). Subsequently, we determined that HA treatment induces the recruitment of a significant amount of PKCε (Fig. 1*A*, *a*, *lane 2*) into the CD44-PKCε complex (Fig. 1*A*, *b*, *lane 2*). Pretreatment of MCF-7 cells with anti-CD44 antibody followed by HA treatment results in a significant reduction of PKCε (Fig. 1*A*, *a*, *lane 3*) in the anti-CD44-immunoprecipitated materials (Fig. 1*A*, *b*, *lane 3*). These findings establish the fact that PKCε is accumulated in a complex with CD44 (in whole cells) following HA treatment of the MCF-7 breast tumor cells.

In addition, we have measured the PKCε kinase activity in the CD44 complex isolated from MCF-7 cells (Fig. 1*B*). The kinase activity was determined by the ability of PKCε to phosphorylate a purified PKC-specific substrate peptide-2 (Fig. 1*B*). Our results indicate that PKCε present in the CD44-associated complex following HA treatment is capable of phosphorylating the PKC substrate peptide-2 (Fig. 1*B*, *bar 2*) to a ~3-fold higher level compared with the controls (*e.g.* CD44-associated PKCε activities detected from MCF-7 cells pretreated with anti-CD44 antibody plus HA or treated with no HA (Fig. 1*B*, *bar 1* and *bar 3*)). These results demonstrate that activation of PKCε is both HA-dependent and CD44-specific in MCF-7 cells.

PKC phosphorylation of cellular proteins plays an important role in regulating tumor cell behaviors (65). Our recent findings indicate that the stem cell marker, Nanog, is closely associated with HA-CD44-mediated tumor cell growth and chemoresistance in MCF-7 cells (5). In searching for a possible linkage between HA-CD44-mediated PKCε signaling and breast tumor cell-specific function, we have demonstrated that CD44-linked PKCε (isolated from MCF-7 cells treated with HA) is capable of phosphorylating Nanog *in vitro* (Fig. 2*A*, *bar 2*). A ~3-fold lower level of Nanog phosphorylation is detected using PKCε isolated from cells that are not treated with HA (Fig. 2*A*, *bar 1 versus bar 2*) or pretreated with anti-CD44 antibody plus HA (Fig. 2*A*, *bar 3 versus bar 2*). Furthermore, we have noted that the ability of PKCε to phosphorylate Nanog is significantly reduced using PKCε isolated from cells treated with PKCε siRNA (but not scrambled sequence siRNA) in the presence or absence of HA (Fig. 2*A*, *bars 4–7*). These findings clearly indicate that Nanog serves as a specific cellular substrate for HA-activated and CD44-linked PKCε (in cell-free systems).

Further *in vivo* analysis indicates that significant Nanog phosphorylation occurs in MCF-7 cells treated with HA for 15 min (Fig. 2*B*, *a* and *b*, *lane 2*). In contrast, Nanog phosphorylation is relatively low in MCF-7 cells without any HA treatment (Fig. 2*B*, *a* and *b*, *lane 1*) or MCF-7 cells pretreated with anti-CD44 antibody followed by HA treatment (Fig. 2*B*, *a* and *b*, *lane 3*). Thus, Nanog phosphorylation is both HA-dependent and CD44-specific. Moreover, we have found that a low level of phosphorylated Nanog is present in MCF-7 cells transfected with scrambled sequence siRNA in the absence of HA treatment (Fig. 2*B*, *a* and *b*, *lane 4*). The unphosphorylated Nanog appears to be localized at the cytosol of MCF-7 cells (Fig. 3, *A–C*). After HA treatment for 15 min in MCF-7 cells (transfected with scrambled sequence siRNA), Nanog becomes highly phosphorylated (Fig. 2*B*, *a* and *b*, *lane 5*) and is also translocated from the cytosol to the nucleus (Fig. 3, *D–F*). Down-regulation of PKCε (by transfecting tumor cells with PKCε siRNA) significantly inhibits HA-CD44-mediated Nanog phosphorylation (Fig. 2*B*, *a* and *b*, *lanes 6* and *7*) and

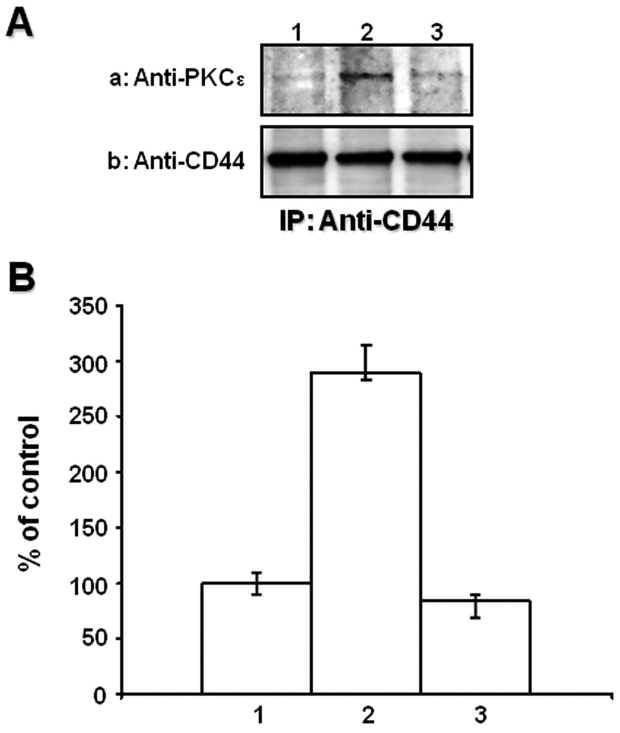

FIGURE 1. **Analyses of HA-induced PKCε-CD44 association and PKCε activity in MCF-7 cells.** Detection of HA-induced PKCε-CD44 complex formation in MCF-7 cells was carried out by solubilizing cells with 1% Nonidet P-40 (Nonidet P-40) buffer, followed by immunoprecipitation (*IP*) and/or immunoblot by anti-CD44 antibody or anti-PKCε antibody, respectively (*A*). Subsequently, CD44-associated PKCε activity using peptide-2 as a substrate was analyzed according to the procedures described under "Materials and Methods." *A*, detection of PKCε in the CD44 complex by anti-CD44-immunoprecipitation, followed by immunoblotting with anti-PKCε antibody (*a*) or reblotting with anti-CD44 (*b*) as a loading control using MCF-7 cells treated with no HA (*lane 1*) or with HA (50 μg/ml) for 10 min (*lane 2*) or pretreated with anti-CD44 followed by a 10-min HA (50 μg/ml) addition (*lane 3*). *B*, peptide-2 phosphorylation by PKCε in cell-free system. The PKCε kinase reaction was performed in the reaction mixture containing [^{32}P]ATP, peptide-2, and CD44-associated PKCε (isolated from MCF-7 cells treated with no HA (*lane 1*) or with a 10-min HA (50 μg/ml) addition (*lane 2*) or pretreated with anti-CD44 antibody followed by a 10-min HA (50 μg/ml) addition (*lane 3*)). Subsequently, the activity of PKCε isolated from these samples was determined by the amount of [^{32}P]ATP incorporated into a PKCε substrate, peptide-2, as described under "Materials and Methods." (The amount of [^{32}P]ATP incorporated into peptide-2 by PKCε isolated from cells treated with no HA (control) is designated as 100%. The values expressed in this figure represent an average of triplicate determinations of four experiments with an S.D. value less than ±5%.)

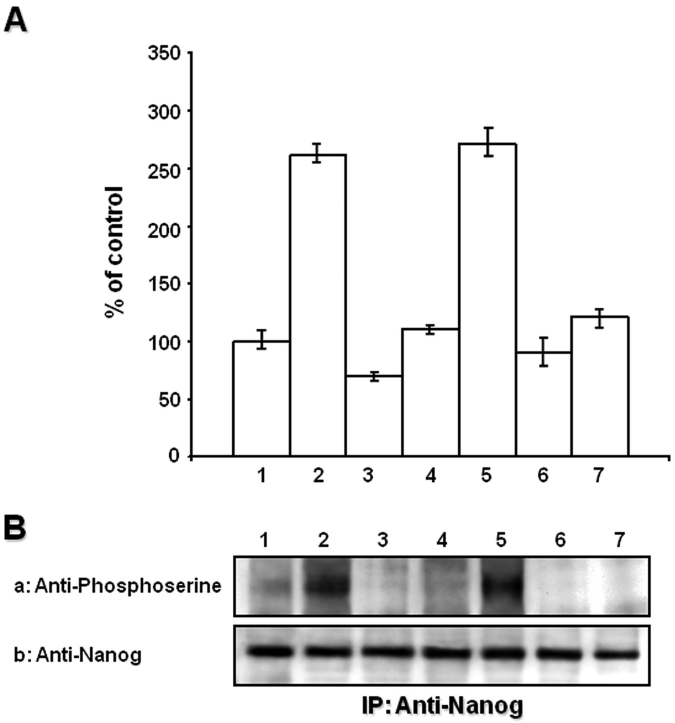

FIGURE 2. **Detection of HA-CD44-mediated Nanog phosphorylation by PKCϵ in cell-free systems and in whole cells.** *A*, Nanog phosphorylation by PKCϵ in a cell-free system. The PKCϵ kinase reaction was carried out in the reaction mixture containing [^{32}P]ATP, purified Nanog, and CD44-associated PKCϵ isolated from MCF-7 cells treated with no HA (*lane 1*), treated with HA for 10 min (*lane 2*), pretreated with anti-CD44 antibody followed by a 10-min HA addition (lane 3), treated with scrambled sequence siRNA (without HA (*lane 4*) or with a 10-min HA addition (*lane 5*)), or treated with PKCϵ siRNA (without HA (*lane 6*) or with a 10-min HA addition (*lane 7*)). Subsequently, the activity of PKCϵ isolated from these samples was determined by the amount of [^{32}P]ATP incorporated into a PKCϵ substrate, Nanog, as described under "Materials and Methods." (The amount of [^{32}P]ATP-incorporated into Nanog by PKCϵ isolated from cells treated with no HA (control) is designated as 100%. The values expressed in this figure represent an average of triplicate determinations of three experiments with an S.D. less than ±5%.) *B*, Nanog phosphorylation in whole cells. Phosphorylation of Nanog was analyzed by solubilizing MCF-7 cells with 1% Nonidet P-40 (Nonidet P-40) buffer, followed by immunoprecipitation (*IP*) with anti-Nanog antibody followed by immunoblotting with anti-phosphoserine antibody (*a*) or anti-Nanog antibody (as a loading control) (*b*), using cell lysates obtained from MCF-7 cells treated with no HA (*lane 1*), treated with HA for 15 min (*lane 2*), pretreated with anti-CD44 followed by a 15-min HA addition (*lane 3*), treated with scrambled sequence siRNA (without HA (*lane 4*) or with HA for 15 min (*lane 5*)), or treated with PKCϵ siRNA (without HA (*lane 6*) or with HA for 15 min (*lane 7*)).

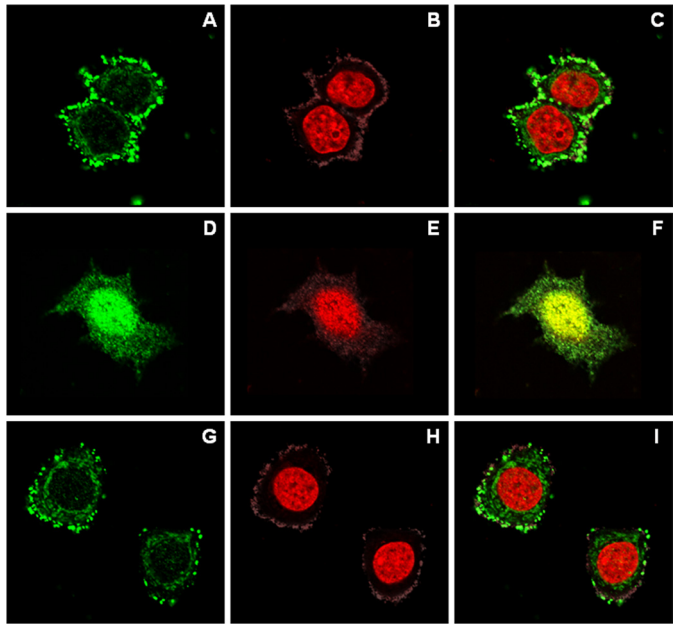

FIGURE 3. **Immunofluorescence staining of Nanog in MCF-7 cells.** MCF-7 cells treated with scrambled sequence siRNA or PKCϵ siRNA (in the presence or absence of HA) were fixed by 2% paraformaldehyde. Subsequently, cells were rendered permeable by ethanol treatment and stained with Nanog and Topro-3 (a nuclear marker), as described under "Materials and Methods." *A–C*, FITC-labeled anti-Nanog (*green*) (*A*), Topro-3 (*red*) (*B*), and an overlay image (*C*) of *A* and *B* in scrambled sequence siRNA-treated cells without an HA addition. *D–F*, FITC-labeled anti-Nanog (*green*) (*D*), Topro-3 (*red*) (*E*), and an overlay image (*F*) of *D* and *E* in scrambled sequence siRNA-treated cells followed by a 15-min HA addition. *G–I*, FITC-labeled anti-Nanog (*green*) (*G*), Topro-3 (*red*) (*H*), and an overlay image (*I*) of *G* and *H* in PKCϵ siRNA-treated cells followed by a 15-min HA addition.

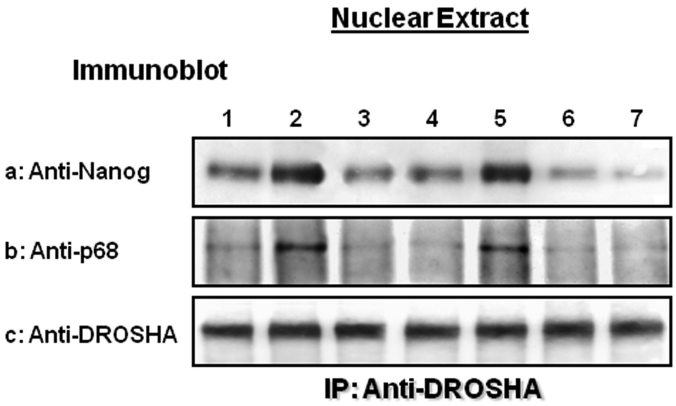

FIGURE 4. **Analyses of HA-CD44-induced Nanog association with p68 and DROSHA in the nuclear fraction of MCF-7 cells.** MCF-7 cells (untreated or treated with PKCϵ siRNA or siRNA with scrambled sequences or pretreated with anti-CD44 antibody) were incubated with HA (50 μg/ml) (or without HA) for 30 min at 37 °C. Nuclear fractions of these cells were then prepared, followed by immunoprecipitation (*IP*) with anti-DROSHA antibody and immunoblotting with anti-Nanog antibody (*a*), anti-p68 antibody (*b*), or anti-DROSHA antibody (as a loading control) (*c*), as described under "Materials and Methods." Nanog association with DROSHA and p68 was detected in MCF-7 cells treated with no HA (*lane 1*), treated with HA for 30 min (*lane 2*), pretreated with anti-CD44, followed by a 30-min HA addition (*lane 3*), treated with scrambled sequence siRNA (without HA (*lane 4*) or with a 30-min HA addition (*lane 5*)) or treated with PKCϵ siRNA (without HA (*lane 6*) or with a 30-min HA addition (*lane 7*)).

nuclear translocation (Fig. 3, *G–I*). These findings indicate that HA-CD44-mediated PKCϵ activation is required for Nanog phosphorylation and nuclear translocation in MCF-7 cells.

Previous studies showed that activated Nanog functions as a transcription factor that translocates from the cytosol to the nucleus, binds to specific promoter elements of target genes, and regulates gene expression of Rex1 and Sox2 (66–68). Here, we report that nuclear translocated Nanog (Fig. 4*a*, *lane 2*) forms a complex with p68 (an RNA helicase) (Fig. 4*b*, *lane 2*) and DROSHA (the nuclear RNase III enzyme) (Fig. 4*c*, *lane 2*) in MCF-7 cells treated with HA. It was also determined that a reduced amount of Nanog-p68-DROSHA complex is detected in tumor cells without HA treatment (Fig. 4, *a–c*, *lane 1*) or pretreated with anti-CD44 antibody followed by HA addition (Fig. 4, *a–c*, *lane 3*). These results indicate that Nanog-p68-DROSHA complex formation requires HA-CD44 interaction.

Further analyses show that the amount of Nanog association with p68 and DROSHA in MCF-7 cells (treated with scrambled

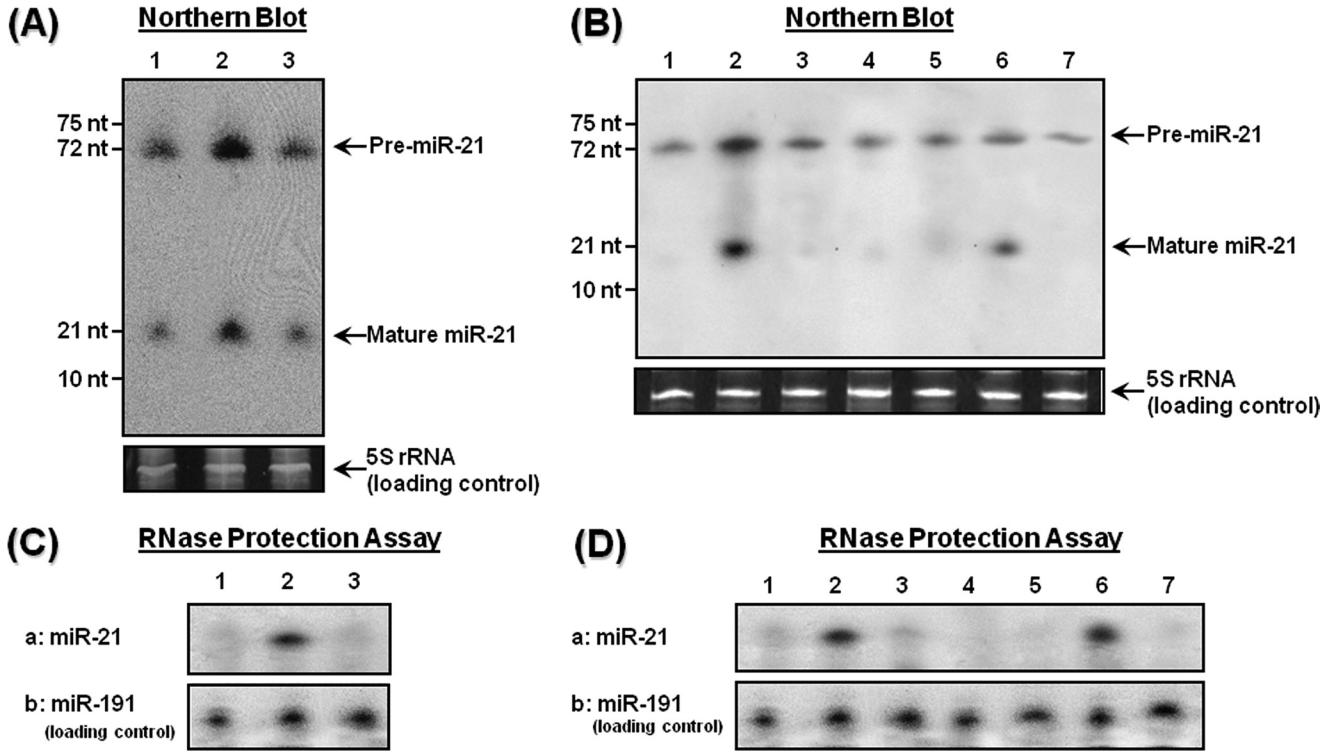

FIGURE 5. **Detection of HA-CD44-induced miR-21 production in MCF-7 cells.** *A* and *B*, detection of both pre-miRNA and mature miR-21 in MCF-7 cells using Northern blot analysis, as described under "Materials and Methods." *A*, autoradiogram of both pre-miRNA and mature miR-21 detected in MCF-7 cells treated with no HA (*lane 1*), treated with HA for 2 h (*lane 2*), or pretreated with anti-CD44, followed by HA addition for 2 h (*lane 3*). *B*, autoradiogram of both pre-miRNA and mature miR-21 detected in MCF cells incubated with scrambled sequence siRNA (without HA (*lane 1*) or with a 2-h HA treatment (*lane 2*)), incubated with PKCϵ siRNA plus a 2-h HA treatment (*lane 3*), incubated with Nanog siRNA plus a 2-h HA treatment (*lane 4*), incubated with miRNA-negative control (without HA (*lane 5*) or with a 2-h HA treatment (*lane 6*)), or incubated with anti-miR-21 inhibitor plus a 2-h HA treatment (*lane 7*). *nt*, nucleotide; 10 and 75 nucleotides were used as miRNA size markers. Ethidium bromide-stained 5 S rRNA in each gel lane was used as a loading control. *C* and *D*, detection of miR-21 in MCF-7 cells using RNase protection assay as described under "Materials and Methods." *C*, autoradiogram of miR-21 detected in MCF-7 cells treated with no HA (*lane 1*), treated with HA for 2 h (*lane 2*), or pretreated with anti-CD44 followed by the addition of HA for 2 h (*lane 3*). *D*, autoradiogram of miR-21 detected in MCF cells incubated with scrambled sequence siRNA (without HA (*lane 1*) or with a 2-h HA treatment (*lane 2*)), incubated with PKCϵ siRNA plus a 2-h HA treatment (*lane 3*), incubated with Nanog siRNA plus a 2-h HA treatment (*lane 4*), incubated with miRNA-negative control (without HA (*lane 5*) or with a 2-h HA treatment (*lane 6*)), or incubated with anti-miR-21 inhibitor plus a 2-h HA treatment (*lane 7*). (An autoradiogram of miR-191 in each gel lane was used as a loading control.)

sequence siRNA) in the presence of HA is higher than in these same complexes from cells without HA treatment (Fig. 4, *a–c*, *lanes 4* and *5*). However, HA-induced stimulation of Nanog complex formation with p68 and DROSHA is strongly inhibited in MCF-7 cells transfected with PKCϵ siRNA (Fig. 4, *a–c*, *lane 6*) or Nanog siRNA, (Fig. 4, *a–c*, *lane 7*). These observations support the notion that HA-CD44-mediated PKCϵ activation and Nanog signaling are closely interacting with p68 (a RNA helicase) and DROSHA (the nuclear RNase III enzyme) in MCF-7 breast tumor cells.

HA-CD44-activated PKCϵ Promotes Nanog-mediated miRNA-21 Production in MCF-7 Cells

The expression of mature miR-21 is detected in various breast cancer-derived cell lines (57) in addition to different tumor cell types. A recent study indicates that both p68 (a RNA helicase) and DROSHA (the nuclear RNase III enzyme) are involved in miR-21 biogenesis (processing the precursor pri-miR-21) in breast tumor cells (55). The question of whether HA-CD44-mediated PKCϵ-Nanog signaling interaction with DROSHA and p68 contributes to an increase in mature miR-21 levels required for oncogenesis and breast tumor progression is the focus of this study.

To test this hypothesis, we first performed a time course experiment to examine the accumulation of pre-miR-21 and mature miR-21 following HA treatment. After extraction of total RNA and isolation of small RNAs, we determined that there was a significant induction of pre-miR-21 (~72 nucleotides) and mature miR-21 (~21 nucleotides) after 2 h of HA treatment by performing Northern Blots with cells that were treated *versus* untreated with HA (Fig. 5*A*, *lanes 1* and *2*). In addition, the mature miR-21 was detected by the *miRVana* miRNA detection kit, which is based on an RNase protection assay. Again, after 2 h of HA treatment, there was a significant increase in the expression of the mature miR-21 (Fig. 5*C*, *lane 2*) compared with that in cells without HA treatment (Fig. 5*C*, *lane 1*). The induction of both the pre-miR-21 and the mature-miR-21 levels was specifically a result of the interaction between HA and the CD44. This was concluded because anti-CD44 antibody plus HA treatment significantly reduced the effect of HA on the expression of mature miR-21, as shown by both Northern blot and RNase protection assay (Fig. 5, *A*, *lane 3*, and *C*, *lane 3*). The increase in miR-21 expression was not due to increased levels of total RNA extracted from each sample, since there were very similar levels of 5 S ribosomal RNA in

both HA-activated and control samples (*e.g.* untreated or pretreated cells followed by HA addition) (Fig. 5*A*). Our results of Northern blot analyses (Fig. 5*B*) and RNase protection assays (Fig. 5*D*) also show that the level of both pre-miR-21 and mature miR-21 production are clearly elevated in MCF-7 cells treated with scrambled sequence siRNA plus HA (Fig. 5, *B* (*lane 2*) and *D* (*lane 2*)), as compared with those cells without HA addition. In contrast, MCF-7 cells treated with either PKCϵ siRNA (Fig. 5, *B* (*lane 3*) and *D* (*lane 3*)) or Nanog siRNA (Fig. 5, *B* (*lane 4*) and *D* (*lane 4*)) contain significantly less HA-induced pre-miR-21 and mature miR-21.

Suppression of breast tumor cells by down-regulating miR-21 was previously accomplished by using an anti-miR-21 inhibitor (69, 70). In this study, we have observed that the expression of both pre-miR-21 and mature miR-21 production can be induced in cells treated with an miRNA-negative control reagent in the presence of HA (Fig. 5*B*, *lane 6 versus lane 5*; Fig. 5*D*, *lane 6 versus lane 5*). Finally, we have confirmed that treatment of MCF-7 cells with a miR-21 inhibitor effectively down-regulates either pre-miR-21 or mature miR-21 production even in the presence of HA (Fig. 5, *B* (*lane 7*) and *D* (*lane 7*)). These observations strongly suggest that HA-CD44-mediated PKCϵ activation and Nanog signaling are tightly linked to the regulation of miR-21 production in MCF-7 cells.

The Effect of HA-CD44-mediated miR-21 (Induced by PKCϵ and Nanog Signaling) on PDCD4 Expression, Anti-apoptosis, and Chemoresistance in Breast Tumor Cells

The array profile of miRNA expression in normal breast tissues *versus* breast carcinoma tissue reveals that miR-21 is abundantly produced in tumors compared with normal tissues (57). The functional significance of miR-21 has been emphasized in several recent studies, and the discovery of its specific targets has also been widely investigated. Previous studies indicate that miR-21 may function as an oncogene and play a role in anti-apoptosis and chemotherapy resistance, in part through down-regulation of several tumor suppressor genes/proteins, including PDCD4 (58, 82). However, the identification of miR-21-specific downstream target(s) and oncogenic event(s) that contributed to HA-CD44-dependent breast tumor cell functions has not been established.

Effect of miR-21 on the Expression of PDCD4 and PDCD4-eIF4A Complex Formation—PDCD4 has been identified as one of the tumor suppressor genes regulated by miR-21 (58, 82). It inhibits translation by forming a complex with the translation initiation factor eIF4A (an RNA helicase) and interfering with the ability of eIF4A to unwind the secondary structure at the 5′-untranslated region of mRNAs (71–73). In this study, we have found that a basal level of PDCD4 and eIF4A expression is present in cells without HA treatment (Fig. 6*A*, *a* and *b*, *lane 1*) or in cells pretreated with anti-CD44 antibody followed by HA treatment (Fig. 6*A*, *a* and *b*, *lane 3*). However, HA treatment promotes down-regulation of the tumor suppressor protein (PDCD4) expression (but not eIF4A expression) in MCF-7 cells (Fig. 6*A*, *a* and *b*, *lane 2*). Thus, the reduction of PDCD4 expression (but not eIF4A) appears to be HA-dependent and CD44-specific in breast tumor cells. Further analyses indicate that a basal level of the PDCD4-eIF4A complex is present in MCF-7

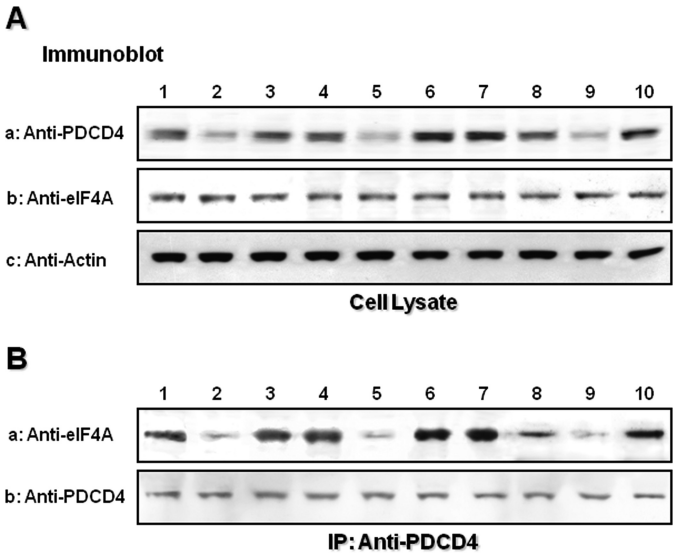

FIGURE 6. **Analyses of HA-CD44-mediated PDCD4-eIF4A expression and PDCD4-eIF4A interaction in MCF-7 cells.** Detection of HA-CD44-induced PDCD4-eIF4A expression in MCF-7 cells was carried out by solubilizing cells with 1% Nonidet P-40 (Nonidet P-40) buffer, followed by immunoblotting with anti-PDCD4 antibody or anti-eIF4A antibody, respectively (*A*). The formation of PDCD4-eIF4A complex was also analyzed by immunoprecipitating the cell lysate with anti-PDCD4 antibody, followed by immunoblotting with anti-eIF4A antibody (*B*), as described under "Materials and Methods." *A*, detection of the expression of PDCD4 or eIF4A by anti-PDCD4-mediated (*a*) or anti-eIF4A-mediated (*b*) immunoblotting using cell lysate isolated from MCF-7 cells treated with no HA (*lane 1*), treated with HA for 24 h (*lane 2*), pretreated with anti-CD44 followed by a 24-h HA addition (*lane 3*), treated with scrambled sequence siRNA (without HA (*lane 3*) or with HA for 24 h (*lane 4*)), treated with PKCϵ siRNA plus HA for 24 h (*lane 6*), treated with Nanog siRNA plus HA for 24 h (*lane 7*), treated with miRNA-negative control (without HA (*lane 8*) or with HA for 24 h (*lane 9*)), or treated with anti-miR-21 inhibitor plus HA for 24 h (*lane 10*). The amount of actin detected by anti-actin-mediated immunoblot in each gel lane was used as a loading control. *B*, detection of the PDCD4-eIF4A complex by anti-PDCD4-mediated immunoprecipitation (*IP*) (*a*), followed by anti-eIF4A-mediated immunoblotting (*b*) (as a loading control) using cell lysate isolated from MCF-7 cells treated with no HA (*lane 1*), treated with HA for 24 h (*lane 2*), pretreated with anti-CD44 followed by a 24-h HA addition (*lane 3*), treated with scrambled sequence siRNA (without HA (*lane 3*) or with HA for 24 h (*lane 4*)), treated with PKCϵ siRNA plus HA for 24 h (*lane 6*), treated with Nanog siRNA plus HA for 24 h (*lane 7*), treated with miRNA-negative control (without HA (*lane 8*) or with HA for 24 h (*lane 9*), or treated with anti-miR-21 inhibitor plus HA for 24 h (*lane 10*).

cells without HA treatment (Fig. 6*B*, *a* and *b*, *lane 1*) or in cells pretreated with anti-CD44 antibody followed by HA treatment (Fig. 6*B*, *a* and *b*, *lane 3*). However, the amount of the PDCD4-eIF4A complex is significantly decreased in MCF-7 cells treated with HA (Fig. 6*B*, *a* and *b*, *lane 2 versus lanes 1* and *3*). These findings indicate that HA-CD44 interaction is required for the regulation of PDCD4 expression and PDCD4-eIF4A interaction in breast tumor cells. We have also confirmed that down-regulation of miR-21 by treating MCF-7 cells with an anti-miR-21 inhibitor (but not a negative control miRNA) promotes up-regulation of PDCD4 expression (but not eIF4A expression) (Fig. 6*A*, *a* and *b*, *lane 10 versus lane 9*) and PDCD4-eIF4A association in the presence of HA (Fig. 6*B*, *a* and *b*, *lane 10 versus lane 9*). These results support the contention that miR-21 (mediated by HA-CD44 binding) is acting as an oncogene by down-regulating the expression of the tumor suppressor, PDCD4, and its interaction with eIF4A. Furthermore, treatment of MCF-7 cells with either PKCϵ siRNA or Nanog siRNA (in the presence of HA) induces an elevated level of

PDCD4 expression (but not eIF4A expression) and PDCD4-eIF4A complex formation (Fig. 6*A*, *a* and *b*, *lanes 6* and *7*; Fig. 6*B*, *a* and *b*, *lanes 6* and *7*). Although a basal level of PDCD4 expression and PDCD4-eIF4A complex was detected in cells treated with scrambled sequence siRNA without HA addition (Fig. 6*A*, *a* and *b*, *lane 4*; Fig. 6*B*, *a* and *b*, *lane 4*), significant reduction of either PDCD4 expression or PDCD4-eIF4A complex was observed in these cells treated with HA (Fig. 6*A*, *a* and *b*, *lane 5*; Fig. 6*B*, *a* and *b*, *lane 5*). These findings indicate that the signaling network consisting of PKCε-Nanog and miR-21 is functionally coupled with the inhibition of the tumor suppressor protein (PDCD4) expression and reduces its association with eIF4A. These effects facilitate the initiation of translation and protein production in HA-CD44-activated breast tumor cells.

Effect of miR-21 on IAPs and MDR1 (P-gp) Expression and Chemotherapeutic Response—To determine how these changes in the tumor suppressor protein (PDCD4) expression and function by miR-21 (via HA-CD44 interaction and PKCε-Nanog signaling) may affect breast tumor cell-specific behaviors (*e.g.* anti-apoptosis and chemoresistance), we decided to analyze the expression of the IAPs and the chemoresistance protein-1 (MDR1/P-gp). The IAPs constitute a family of at least nine proteins, including XIAP and survivin, that block apoptosis by direct binding to caspases (74). Overexpression of IAPs (*e.g.* XIAP and survivin) is thought to be linked to chemoresistance by suppressing apoptosis (75–77). MDR1 (P-gp) belongs to the ATP-binding cassette transporters, a superfamily of channel proteins (78–81). The functions of MDR1 (P-gp) include the efflux and retention of ions, nutrients, lipids, amino acids, peptides, proteins, and drugs (78–81). HA-CD44 interaction has been shown to induce the expression of survivin and MDR1/P-gp in tumor cells (5, 6, 42, 45). The question of whether miR-21 (induced by HA-CD44 interaction and PKCε-Nanog signaling) regulates the expression of IAPs (*e.g.* XIAP and survivin) and MDR1 in breast tumor cells has not been investigated previously.

To answer this question, immunoblot analyses using a panel of antibodies (*e.g.* anti-XIAP antibody, anti-survivin antibody, and anti-MDR1/P-gp antibody) were employed to detect the production of three proteins: survivin, XIAP, and MDR1 (P-gp) in MCF-7 cells. Our data indicate that the expression of both IAPs (*e.g.* XIAP and survivin) and MDR1/P-gp are significantly increased in MCF-7 treated with HA (Fig. 7, *a–c*, *lane 2 versus lane 1*). In contrast, these three proteins (*e.g.* XIAP, survivin, and MDR1/P-gp) are present in relatively low amounts in MCF-7 cells treated with no HA (Fig. 7, *a–c*, *lane 1 versus lane 2*) or in those cells pretreated with anti-CD44 antibody followed by HA addition (Fig. 7, *a–c*, *lane 3 versus lane 2*). These findings support the notion that the expression of IAPs and MDR1 is both HA- and CD44-dependent. Most importantly, down-regulation of miR-21 by treating cells with an anti-miR-21 inhibitor significantly attenuates the HA-CD44-activated expression of IAPs (*e.g.* XIAP and survivin) and MDR1/P-gp (Fig. 7, *a–c*, *lane 10*). In contrast, MCF-7 cells treated with a miRNA-negative control are capable of inducing the expression of both IAPs (*e.g.* XIAP or survivin) and MDR1/P-gp in the presence of HA (Fig. 7, *a–c*, *lanes 8* and *9*). Furthermore, we have observed that

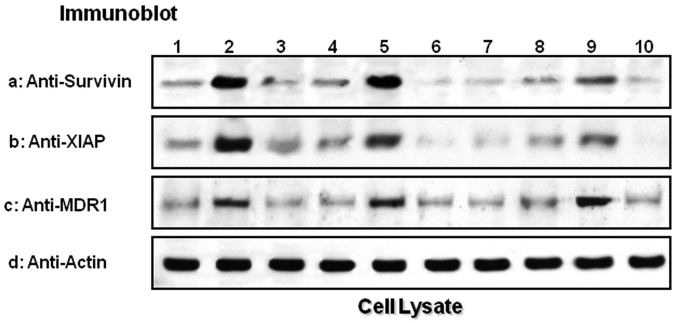

FIGURE 7. **Detection of HA-CD44-induced expression of survivin, XIAP, and MDR1 (P-gp) in MCF-7 cells.** Cell lysates isolated from MCF-7 cells treated with no HA (*lane 1*), treated with HA for 24 h (*lane 2*), pretreated with anti-CD44 followed by a 24-h HA addition (*lane 3*), treated with scrambled sequence siRNA (without HA (*lane 4*) or with HA for 24 h (*lane 5*)), treated with PKCε siRNA plus HA for 24 h (*lane 6*), treated with Nanog siRNA plus HA for 24 h (*lane 7*), treated with miRNA-negative control (without HA (*lane 8*) or with HA for 24 h (*lane 9*)), or treated with anti-miR-21 inhibitor plus HA for 24 h (*lane 10*) were processed for immunoblotting using anti-survivin antibody (*a*), anti-XIAP antibody (*b*), anti-MDR1 (P-gp) antibody (c), or anti-actin antibody (as a loading control) (*d*), respectively, as described under "Materials and Methods."

the expression of IAPs (*e.g.* XIAP and survivin) and MDR1/P-gp are significantly inhibited when MCF-7 cells were pretreated with PKCε siRNA or Nanog siRNA (Fig. 7, *a–c*, *lanes 6* and *7*) but not scrambled sequence siRNA followed by HA addition (Fig. 7, *a–c*, *lanes 4* and *5*), respectively. The fact that down-regulation of both PKCε-Nanog signaling and miR-21 production inhibits the expression of IAPs (*e.g.* XIAP and survivin) and MDR1/P-gp indicates that the HA-CD44-activated PKCε-Nanog signaling and miR-21 function actively participate in the up-regulation of IAPs and MDR1/P-gp in breast tumor cells.

To further assess whether the chemotherapeutic drug responses of MCF-7 cells might be regulated by the HA-CD44 interaction with PKCε-Nanog signaling and miR-21 production, we performed tumor cell growth and apoptosis assays using two anti-breast cancer chemotherapeutic drugs (*e.g.* doxorubicin and paclitaxel (Taxol)) in the presence or absence of HA or anti-CD44 antibody plus HA. In the absence of HA, doxorubicin-treated MCF-7 cells displayed an increase of apoptotic tumor cells and a low level of tumor cell survival with IC_{50} values of 60 nM (Tables 1 and 2). Paclitaxel-treated MCF-7 cells also exhibit a relatively high level of apoptosis and a low level of tumor cell survival, with IC_{50} values of ~40 nM (Tables 1 and 2). However, the addition of HA enhances cell survival and reduces apoptosis in untreated controls (*i.e.* without chemotherapeutic drugs) and decreases the ability of both doxorubicin (IC_{50} of 320 nM) and paclitaxel (IC_{50} of 160 nM) to induce tumor apoptosis and cell death (Tables 1 and 2). These observations strongly suggest that HA causes a decrease in apoptosis and an increase in tumor cell survival, leading to the enhancement of chemoresistance to both doxorubicin and paclitaxel treatment (Tables 1 and 2). Furthermore, pretreatment of these tumor cells with anti-CD44 antibody followed by HA addition significantly increases tumor cell apoptosis and reduces the HA-mediated drug resistance (Table 1 and 2). This result indicates that HA-CD44 interaction promotes anti-apoptosis and cell survival in the presence of chemotherapeutic drugs, such as doxorubicin and paclitaxel, in breast tumor cells. Moreover,

TABLE 1

IC_{50} analyses of doxorubicin and paclitaxel in MCF-7 cell growth

IC_{50} is designated as the concentration (nM) of chemotherapeutic drugs (e.g., doxorubicin or paclitaxel) that causes 50% inhibition of tumor cell growth. IC_{50} values are presented as the means ± S.D. All assays consisted of at least six replicates and were performed on at least three different experiments.

Treatments	Doxorubicin (IC_{50})		Paclitaxel (IC_{50})	
	Without HA	With HA	Without HA	With HA
	nM		nM	
Effects of anti-CD44 antibody on the IC_{50} of doxorubicin and paclitaxel in HA-mediated MCF-7 cell growth				
Untreated cells (control)	60 ± 5	320 ± 14	64 ± 8	160 ± 15
Normal rat IgG-treated cells	58 ± 6	298 ± 12	51 ± 14	152 ± 17
Rat anti-CD44-treated cells	50 ± 4	55 ± 6	22 ± 4	20 ± 5
Effects of PKCε siRNA and Nanog siRNA on the IC_{50} of doxorubicin and paclitaxel in HA-mediated MCF-7 cell growth				
Scrambled siRNA- treated cells	65 ± 5	350 ± 15	46 ± 10	180 ± 20
PKCε siRNA-treated cells	42 ± 3	49 ± 3	28 ± 3	32 ± 5
Nanog siRNA-treated cells	40 ± 6	52 ± 5	29 ± 4	30 ± 6
Effects of anti-miR-21 inhibitor on the IC_{50} of doxorubicin and paclitaxel in HA-mediated MCF-7 cell growth				
miRNA-negative control-treated cells	60 ± 4	324 ± 10	40 ± 10	165 ± 12
Anti-miR-21 inhibitor-treated cells	40 ± 3	52 ± 6	38 ± 3	46 ± 6

TABLE 2

Analyses of multidrug-induced apoptosis in MCF-7 cells

Cells were designated apoptotic when displaying Annexin V-positive staining. In each sample, at least 500 cells from five different fields were counted, with the percentage of apoptotic cells calculated as Annexin V-positive cells/total number of cells. The values are presented as the means ± S.D.

Treatments	Apoptotic cells (Annexin V-positive cells/total cells × 100%)		
	No Drug	With doxorubicin	With paclitaxel
Effects of HA on multidrug-induced apoptosis in MCF-7 cells			
Untreated cells (control)	1.2 ± 0.4	44.2 ± 2.5[a]	37.3 ± 3.0[a]
HA-treated cells	1.0 ± 0.2[a]	15.6 ± 2.2[a]	14.7 ± 2.5[a]
Effects of PKCε siRNA and Nanog siRNA on multidrug-induced apoptosis in MCF-7 cells			
Scrambled siRNA- treated cells (no HA)	2.5 ± 0.6	43.2 ± 3.6[b]	48.1 ± 2.8[b]
Scrambled siRNA-treated cells (with HA)	2.0 ± 0.7[b]	22.6 ± 2.5[b]	23.5 ± 1.3[b]
PKCε siRNA-treated cells (no HA)	14.5 ± 2.2[b]	65.4 ± 6.7[b]	61.2 ± 3.6[b]
PKCε siRNA-treated cells (with HA)	16.0 ± 2.3[b]	58.0 ± 3.9[b]	56.2 ± 2.8[b]
Nanog siRNA-treated cells (no HA)	14.9 ± 3.6[b]	65.1 ± 4.8[b]	62.3 ± 5.5[b]
Nanog siRNA-treated cells (+ HA)	15.0 ± 1.4[b]	59.4 ± 3.7[b]	56.2 ± 4.8[b]
Effects of anti-miR-21 inhibitor on multidrug-induced apoptosis in MCF-7 cells			
miRNA-negative control-treated cells (no HA)	2.3 ± 0.8	40.2 ± 3.3[c]	49.7 ± 1.9[c]
miRNA-negative control-treated cells (with HA)	1.8 ± 0.5[c]	21.1 ± 3.2[c]	22.5 ± 2.0[c]
Anti-miR-21 inhibitor-treated cells (no HA)	15.0 ± 2.4[c]	62.4 ± 3.3[c]	59.7 ± 2.3[c]
Anti-miR-21 inhibitor-treated cells (with HA)	14.8 ± 3.3[c]	59.1 ± 4.0[c]	54.1 ± 2.4[c]

[a] Significantly different ($p < 0.001$; analysis of variance; $n = 4$) as compared with untreated (no drug treatment and no HA addition) (control) samples.
[b] Significantly different ($p < 0.005$; analysis of variance; $n = 5$) as compared with scrambled sequence-treated (no drug and no HA addition) (control) samples.
[c] Significantly different ($p < 0.005$; analysis of variance; $n = 5$) as compared with miRNA-negative control-treated (no drug and no HA addition) (control) samples.

down-regulation of PKCε, Nanog, or miR-21 (by transfecting tumor cells with PKCε siRNA or Nanog siRNA or anti-miR-21 inhibitor (but not scrambled sequence siRNA or an miRNA-negative control)) effectively attenuates HA-mediated tumor cell anti-apoptosis/survival and enhances multidrug sensitivity in MCF-7 cells (Tables 1 and 2). Together, these findings indicate that the HA-CD44-mediated PKCε-Nanog signaling pathways and miR-21 function provide new drug targets to sensitize tumor cells to undergo apoptosis/death and to overcome chemotherapy resistance in breast cancer cells.

DISCUSSION

Chemotherapy resistance is one of the primary causes of morbidity in patients diagnosed with solid tumors, such as breast cancer (1–3). It is now certain that a number of oncogenic signaling pathways are closely involved with multidrug-resistant phenotypes (4–6). In particular, HA-CD44-activated cancer cells have been strongly implicated in the development of chemoresistance (5, 6, 42–48). Specifically, HA is capable of stimulating MDR1 (P-gp) expression and drug resistance in breast tumor cells (5, 6). CD44 also interacts with MDR1 (P-gp) to promote cell migration and invasion of breast tumor cells (83). Previously, we have reported that activation of HA-CD44-mediated oncogenic signaling events (*e.g.* intracellular Ca^{2+} mobilization, epidermal growth factor receptor-mediated ERK signaling, topoisomerase activation, and ankyrin-associated cytoskeleton function) leads to multidrug resistance in a variety of tumor cells (5, 46–48).

Recently, we have found that the stem cell marker Nanog appears to be closely involved in HA-CD44-mediated chemoresistance in breast tumor cells (5). Nanog is an important transcription factor involved in the self-renewal and maintenance of pluripotency in the inner cell mass of embryos and embryonic stem cells (84). Nanog signaling is regulated by interactions among various pluripotent stem cell regulators

(*e.g.* Rex1, Sox2, and Oct3/4), which together control the expression of a set of target genes required for embryonic stem cell pluripotency (66, 85). These findings confirm the essential role of Nanog in regulating a variety of cellular functions. Both breast carcinomas and breast tumor cells have been shown to express several common embryonic stem cell markers, including Nanog (86). The Nanog family of proteins functions as growth-promoting regulators by up-regulating transcriptional activities and gene expression in breast tumor cells (87). It is not well understood how Nanog signaling is regulated by HA-CD44 interaction, which causes chemoresistance in breast tumor cells.

Both HA and CD44 are important activators of oncogenesis and chemoresistance in breast tumor cells (4–6, 42–48). It has been well documented that the external portion of CD44 binds to HA, whereas the intracellular domain of CD44 interacts with receptor kinases (*e.g.* ErbB2, epidermal growth factor receptor, and TGFβ receptors) and non-receptor kinases (*e.g.* c-Src and ROK) (28–34). HA-induced CD44 interaction with these kinases plays a pivotal role in promoting breast tumor cell functions (28–34). Previous studies indicated that the cytoplasmic domain of CD44 can be phosphorylated by PKC (61, 62). Most importantly, CD44 phosphorylation by PKC promotes ankyrin binding to CD44 and stimulates a number of biological activities (61, 62). These findings indicate that CD44-cytoskeleton interaction and PKC signaling are closely coupled. Based on structural features and activation requirements, the PKC family of proteins has been divided into at least three groups of isoforms: the classical isoforms (α, βI, βII, and γ); the novel isoforms (δ, ϵ, θ, and η); and the atypical isoforms (ζ and ι/λ) (36). In particular, PKCϵ appears to play a causative role in establishing breast tumor cell-specific phenotypes (37–39). PKCϵ also acts as an anti-apoptotic protein and protects breast cancer MCF-7 cells from tumor necrosis factor-α-mediated apoptosis, in part through inhibition of Bax activation and translocation to the mitochondria (88).

In addition, PKCϵ is known to function as a transforming oncogene by interacting with several signaling components, including RhoA/C, Stat-3, and Akt (35). In this study, we have found that HA binding to breast tumor cells (MCF-7 cells) not only recruits PKCϵ into CD44 complexes but also activates its enzymatic activities (Fig. 1). Most importantly, we have determined that Nanog serves as one of cellular substrates for HA-CD44-activated PKCϵ (Fig. 2). Nanog has been shown to regulate the expression of pri-miRNA by associating to the 5′-regulatory region of the miRNAs that are involved in the most critical molecular processes during development (56). Our data indicate that PKCϵ-activated Nanog is translocated from the cytosol to the nucleus (Fig. 3) and forms a complex with DROSHA/p68 (Fig. 4), resulting in miR-21 production in HA-CD44-activated breast tumor cells (Fig. 5). The fact that down-regulation of either PKCϵ or Nanog (by transfecting cells with either PKCϵ siRNA or Nanog siRNA) not only abolishes Nanog association with DROSHA and p68 (Fig. 4) but also inhibits miR-21 production (Fig. 5) in HA-treated MCF-7 cells clearly indicates the importance of PKCϵ signaling and Nanog function in regulating HA-CD44-regulated miR-21 production.

Our results are consistent with previous reports showing association of DROSHA/p68 microprocessor complex with certain signaling regulators during miRNA production. For example, it has been shown that there is a molecular interaction between p53 and the DROSHA complex in HCT116 cells. This interaction with the processing complex occurs via the RNA helicases (p68/p72) (59). It is also noted that activation of the TGFβ-mediated SMAD-2 signaling stimulates the expression of a subset of miRNAs, including miR-21 (55). Specifically, this TGFβ-mediated signaling event occurs at a post-translational step promoting the processing of primary transcripts of miR-21 (pri-miR-21) into precursor miR-21 (pre-miR-21) by DROSHA complex (55). TGFβ-specific SMAD-2 signaling transducer also becomes recruited to pri-miR-21 in a complex with p68 (the RNA helicase), components of the DROSHA microprocessor complex in human vascular smooth muscle cells (55). Apparently, the DROSHA/p68 microprocessor complex is closely associated with the production of miRNAs, such as miR-21, by a variety of signaling pathways. Since miR-21 has been shown to participate in breast cancer progression (57), the elucidation (in this study) of HA-CD44 signaling pathway-specific mechanisms involved with miR-21 biogenesis is significant for the formulation of future intervention strategies for treating breast cancer.

The ability of certain chemotherapeutic agents (*e.g.* doxorubicin and paclitaxel) to induce tumor cell death is often counteracted by the presence of anti-apoptotic proteins, leading to chemoresistance (75–77). Several lines of evidence point toward the IAP family (*e.g.* survivin and XIAP) playing a role in oncogenesis via their effective suppression of apoptosis (74). The mode of action of IAPs in suppressing apoptosis appears to be through direct inhibition of caspases and procaspases (primarily caspase 3 and 7) (74). IAPs also support chemoresistance by preventing tumor cell death induced by anticancer agents (75–77). Although certain anti-apoptotic proteins (*e.g.* Bcl-xL) have been shown to participate in anti-apoptosis and chemoresistance in HA-CD44-activated breast tumor cells (6), the involvement of IAPs in HA-CD44-mediated tumor cell survival and chemoresistance has not been fully elucidated. Multidrug resistance can also be mediated by overexpression of MDR1 (P-gp) (41), which functions as a drug efflux pump actively reducing intracellular drug concentrations in resistant tumor cells (5, 41). Previous studies showed that HA-CD44 induces the expression of MDR1 (P-gp) and chemoresistance in breast tumor cells (5, 6, 42–48). In the present study, we have made several important and novel observations. Specifically, our results indicate that HA-CD44-mediated PKCϵ-Nanog signaling mediates miR-21 production, which in turn, exerts its influence on tumor cell-specific functions, including anti-apoptosis and chemoresistance (Fig. 7 and Tables 1 and 2).

Furthermore, miR-21 down-regulation has been shown to be effective in blocking oncogenesis by up-regulating its known targets, including tumor suppressor proteins, such as PDCD4 (58). In fact, loss of PDCD4 expression occurs during breast tumor progression (89, 90). Up-regulation of PDCD4 is closely linked to apoptosis and translation inhibition (via its binding and inhibiting the helicase activity of eIF4A, a component of translation initiation complex) (71–73). In this study, we have

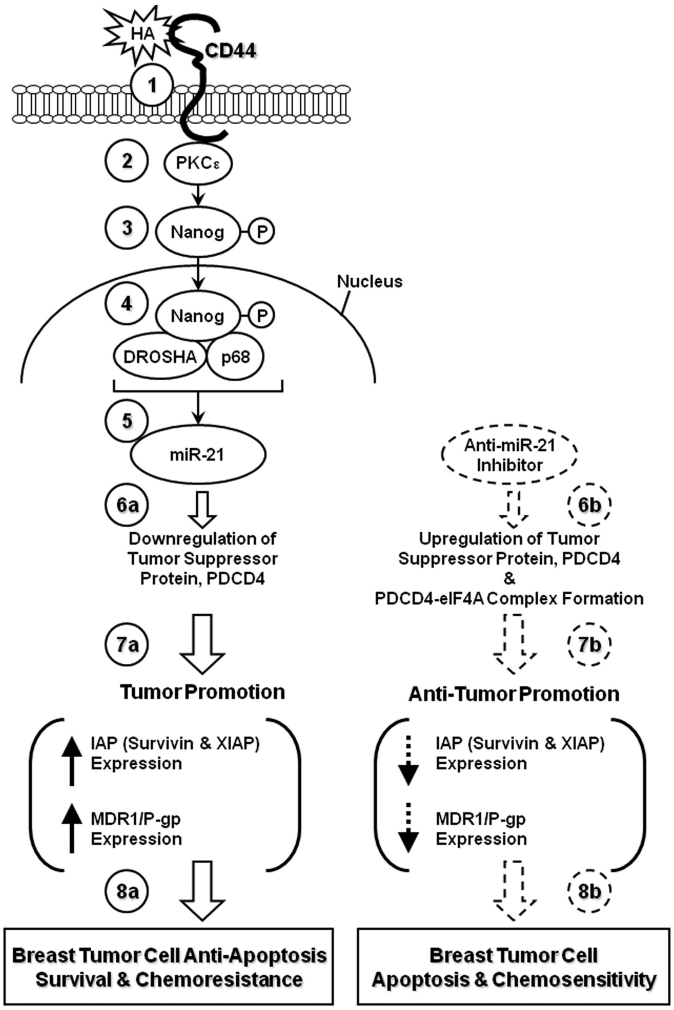

FIGURE 8. **A proposed model for HA-CD44-mediated PKCϵ activation and Nanog signaling in the regulation of miRNA-21 production, oncogenesis, and chemoresistance in breast tumor cells.** The binding of HA to CD44 (*step 1*) promotes PKCϵ activity (*step 2*), which, in turn, causes phosphorylation of Nanog (*step 3*). Phosphorylated Nanog then translocates from the cytosol to the nucleus and interacts with the microprocessor complex containing the RNase III (DROSHA) and the RNA helicase (p68) (*step 4*), resulting in miR-21 production (*step 5*). The resultant miR-21 then functions to down-regulate the tumor suppressor protein (PDCD4) (*step 6a*; indicated by the *arrow* with *solid lines*) and promotes oncogenesis (*step 7a*; indicated by the *arrow* with *solid lines*), leading to IAP (survivin and XIAP)/MDR1 (P-gp) expression, breast tumor cell anti-apoptosis/survival, and chemoresistance (*step 8a*; indicated by the *arrow* with *solid lines*). In direct contrast, treatment of breast tumor cells with an anti-miR-21 inhibitor (indicated by the *arrow* with *dashed lines*) induces tumor suppressor protein (PDCD4) up-regulation and PDCD4-eIF4A complex formation, which then inhibits translational machinery (*step 6b*; indicated by the *arrow* with *dashed lines*). Subsequently, these changes result in the inhibition of IAP (survivin and XIAP) and MDR1 expression (*step 7b*; indicated by the *arrow* with *dashed lines*), stimulation of apoptosis/cell death, and enhancement of chemosensitivity (*step 8b*; indicated by the *arrow* with *dashed lines*) in breast tumor cells. This newly discovered PKCϵ-Nanog signaling pathway leading to miR-21 functioning should provide important drug targets for sensitizing tumor cell apoptosis and overcoming chemoresistance in HA-CD44-activated breast cancer cells.

demonstrated that HA-CD44-activated PKCϵ-Nanog signaling and miR-21 reduces PDCD4 expression (Fig. 6), resulting in oncogenesis (by enhancing the expression of IAP and MDR1/P-gp) (Fig. 7). Furthermore, down-regulation of HA-CD44-activated PKCϵ-Nanog signaling (by PKCϵ siRNA-Nanog siRNA) and miR-21 production (by anti-miR-21 inhibitor) not only induces PDCD4 up-regulation and PDCD4-eIF4A complex (Fig. 6) but also inhibits the expression of survival proteins (*e.g.* survivin and XIAP) and MDR1/P-gp (Fig. 7). Subsequently, these signaling perturbation events contribute to apoptosis and chemosensitivity (Tables 1 and 2). These findings clearly establish causal links between PKCϵ-Nanog signaling and miR-21 function, including PDCD4 down-regulation, anti-apoptosis, and chemoresistance.

Another known cellular target for miR-21 is the tumor suppressor gene *PTEN* (phosphatase and tensin homologue deleted on chromosome 10; 10q23.3) (91). In particular, miR-21 has been shown to be involved in the promotion of cell invasion, migration, and growth through the repression of *PTEN* and activation of phosphatidylinositol 3-kinase-AKT signaling (91). Previous studies demonstrated that HA-CD44-mediated phosphatidylinositol 3-kinase-AKT signaling plays a key role in regulating oncogenesis and chemoresistance (34, 44, 45). The relationship between miR-21-mediated *PTEN* repression and phosphatidylinositol 3-kinase-AKT-associated chemoresistance during HA-CD44 signaling in breast tumor cells is currently under investigation in our laboratory.

As summarized in Fig. 8, we propose that HA binding to CD44 (*step 1*) promotes PKCϵ activity (*step 2*), which, in turn, causes phosphorylation of Nanog (*step 3*). Phosphorylated Nanog then translocates from the cytosol to the nucleus and interacts with the microprocessor complex containing the RNase III (DROSHA) and the RNA helicase (p68) (*step 4*), resulting in miR-21 production (*step 5*). The resultant miR-21 then functions to down-regulate the tumor suppressor protein (PDCD4) (*step 6a*) and promotes oncogenesis (*step 7a*), leading to IAP (survivin and XIAP)/MDR1 (P-gp) expression, breast tumor cell anti-apoptosis/survival, and chemoresistance (*step 8a*). In direct contrast, treatment of breast tumor cells with an anti-miR-21 inhibitor induces tumor suppressor protein (PDCD4) up-regulation and PDCD4-eIF4A complex formation, which then inhibits translational machinery (*step 6b*). Subsequently, these changes result in the inhibition of IAP (survivin and XIAP) and MDR1 expression (*step 7b*), stimulation of apoptosis/cell death, and enhancement of chemosensitivity (*step 8b*) in breast tumor cells. This newly discovered PKCϵ-Nanog signaling pathway leading to miR-21 functioning should provide important drug targets for sensitizing tumor cell apoptosis and overcoming chemoresistance in HA-CD44-activated breast cancer cells.

Acknowledgments—We gratefully acknowledge the assistance of Drs. Gerard J. Bourguignon and Walter M. Holleran in the preparation and review of the manuscript. We are grateful for Christina Camacho for assistance in preparing graphs and illustrations. We also thank Christine Earle for help in preparing HA reagent.

REFERENCES

1. Kuo, M. T. (2007) *Adv. Exp. Med. Biol.* **608,** 23–30
2. Chuthapisith, S., Eremin, J. M., El-Sheemy, M., and Eremin, O. (2006) *Surgeon* **4,** 211–219
3. Lønning, P. E. (2003) *Lancet Oncol.* **4,** 177–185
4. Bourguignon, L. Y. (2008) *Semin. Cancer Biol.* **18,** 251–259
5. Bourguignon, L. Y., Peyrollier, K., Xia, W., and Gilad, E. (2008) *J. Biol. Chem.* **283,** 17635–17651

6. Bourguignon, L. Y., Xia, W., and Wong, G. (2009) *J. Biol. Chem.* **284,** 2657–2671
7. Smith, H. S., Stern, R., Liu, E., and Benz, C. (1991) *Basic Life Sci.* **57,** 329–340
8. Bourguignon, L. Y. (2001) *J. Mammary Gland. Biol. Neoplasia* **6,** 287–297
9. Laurent, T. C., and Fraser, J. R. (1992) *FASEB J.* **6,** 2397–2404
10. Lee, J. Y., and Spicer, A. P. (2000) *Curr. Opin. Cell Biol.* **12,** 581–586
11. Weigel, P. H., Hascall, V. C., and Tammi, M. (1997) *J. Biol. Chem.* **272,** 13997–14000
12. Itano, N., and Kimata, K. (1998) *Trends Glycosci. Glycotechnol.* **10,** 23–28
13. Itano, N., and Kimata, K. (1996) *J. Biol. Chem.* **271,** 9875–9878
14. Spicer, A. P., and Nguyen, T. K. (1999) *Biochem. Soc. Trans.* **27,** 109–115
15. Zhang, L., Underhill, C. B., and Chen, L. (1995) *Cancer Res.* **55,** 428–433
16. Stern, R., and Jedrzejas, M. J. (2006) *Chem. Rev.* **106,** 818–839
17. Bourguignon, L. Y., Singleton, P. A., Diedrich, F., Stern, R., and Gilad, E. (2004) *J. Biol. Chem.* **279,** 26991–27007
18. Haylock, D. N., and Nilsson, S. K. (2006) *Regen. Med.* **1,** 437–445
19. Toole, B. P., Wight, T. N., and Tammi, M. I. (2002) *J. Biol. Chem.* **277,** 4593–4596
20. Delpech, B., Chevallier, B., Reinhardt, N., Julien, J. P., Duval, C., Maingonnat, C., Bastit, P., and Asselain, B. (1990) *Int. J. Cancer* **46,** 388–390
21. Kalish, E., Iida, N., Moffat, F. L., and Bourguignon, L. Y. (1999) *Front. Biosci.* **4,** 1–8
22. Iida, N., and Bourguignon, L. Y. (1995) *J. Cell Physiol.* **162,** 127–133
23. Iida, N., and Bourguignon, L. Y. (1997) *J. Cell Physiol.* **171,** 152–160
24. Bourguignon, L. Y., Gunja-Smith, Z., Iida, N., Zhu, H. B., Young, L. J., Muller, W. J., and Cardiff, R. D. (1998) *J. Cell Physiol.* **176,** 206–215
25. Screaton, G. R., Bell, M. V., Jackson, D. G., Cornelis, F. B., Gerth, U., and Bell, J. I. (1992) *Proc. Natl. Acad. Sci. U.S.A.* **89,** 12160–12164
26. Screaton, G. R., Bell, M. V., Bell, J. I., and Jackson, D. G. (1993) *J. Biol. Chem.* **268,** 12235–12238
27. Al-Hajj, M., Wicha, M. S., Benito-Hernandez, A., Morrison, S. J., and Clarke, M. F. (2003) *Proc. Natl. Acad. Sci. U.S.A.* **100,** 3983–3988
28. Bourguignon, L. Y. (2009) in *Hyaluronan in Cancer Biology* (Stern, R., ed) pp. 89–101, Elsevier Publication Co., San Diego, CA
29. Bourguignon, L. Y., Zhu, H., Chu, A., Iida, N., Zhang, L., and Hung, M. C. (1997) *J. Biol. Chem.* **272,** 27913–27918
30. Bourguignon, L. Y., Zhu, H., Shao, L., Zhu, D., and Chen, Y. W. (1999) *Cell Motil. Cytoskeleton* **43,** 269–287
31. Bourguignon, L. Y., Zhu, H., Shao, L., and Chen, Y. W. (2001) *J. Biol. Chem.* **276,** 7327–7336
32. Bourguignon, L. Y., Zhu, H., Zhou, B., Diedrich, F., Singleton, P. A., and Hung, M. C. (2001) *J. Biol. Chem.* **276,** 48679–48692
33. Bourguignon, L. Y., Singleton, P. A., Zhu, H., and Zhou, B. (2002) *J. Biol. Chem.* **277,** 39703–39712
34. Bourguignon, L. Y., Singleton, P. A., Zhu, H., and Diedrich, F. (2003) *J. Biol. Chem.* **278,** 29420–29434
35. Gorin, M. A., and Pan, Q. (2009) *Mol. Cancer* **8,** 9–16
36. Stabel, S., and Parker, P. J. (1991) *Pharmacol. Ther.* **51,** 71–95
37. Steinberg, R., Harari, O. A., Lidington, E. A., Boyle, J. J., Nohadani, M., Samarel, A. M., Ohba, M., Haskard, D. O., and Mason, J. C. (2007) *J. Biol. Chem.* **282,** 32288–32297
38. Pardo, O. E., Wellbrock, C., Khanzada, U. K., Aubert, M., Arozarena, I., Davidson, S., Bowen, F., Parker, P. J., Filonenko, V. V., Gout, I. T., Sebire, N., Marais, R., Downward, J., and Seckl, M. J. (2006) *EMBO J.* **25,** 3078–3088
39. Basu, A., Mohanty, S., and Sun, B. (2001) *Biochem. Biophys. Res. Commun.* **280,** 883–891
40. Hofmann, J. (2004) *Curr. Cancer Drug Targets* **4,** 125–146
41. Baker, E. K., and El-Osta, A. (2004) *Cancer Biol. Ther.* **3,** 819–824
42. Cordo Russo, R. I., García, M. G., Alaniz, L., Blanco, G., Alvarez, E., and Hajos, S. E. (2008) *Int. J. Cancer* **122,** 1012–1018
43. Ohashi, R., Takahashi, F., Cui, R., Yoshioka, M., Gu, T., Sasaki, S., Tominaga, S., Nishio, K., Tanabe, K. K., and Takahashi, K. (2007) *Cancer Lett.* **252,** 225–234
44. Misra, S., Ghatak, S., Zoltan-Jones, A., and Toole, B. P. (2003) *J. Biol. Chem.* **278,** 25285–25288
45. Misra, S., Ghatak, S., and Toole, B. P. (2005) *J. Biol. Chem.* **280,** 20310–20315
46. Wang, S. J., and Bourguignon, L. Y. (2006) *Arch. Otolaryngol. Head Neck Surg.* **132,** 19–24
47. Wang, S. J., and Bourguignon, L. Y. (2006) *Arch. Otolaryngol. Head Neck Surg.* **132,** 771–778
48. Wang, S. J., Peyrollier, K., and Bourguignon, L. Y. (2007) *Arch. Otolaryngol. Head Neck Surg.* **133,** 281–288
49. Cowland, J. B., Hother, C., and Grønbaek, K. (2007) *APMIS* **115,** 1090–1106
50. Cai, X., Hagedorn, C. H., and Cullen, B. R. (2004) *RNA* **10,** 1957–1966
51. Valencia-Sanchez, M. A., Liu, J., Hannon, G. J., and Parker, R. (2006) *Genes Dev.* **20,** 515–524
52. Giraldez, A. J., Cinalli, R. M., Glasner, M. E., Enright, A. J., Thomson, J. M., Baskerville, S., Hammond, S. M., Bartel, D. P., and Schier, A. F. (2005) *Science* **308,** 833–838
53. Salzman, D. W., Shubert-Coleman, J., and Furneaux, H. (2007) *J. Biol. Chem.* **282,** 32773–32779
54. de la Cruz, J., Kressler, D., and Linder, P. (1999) *Trends Biochem. Sci.* **24,** 192–198
55. Davis, B. N., Hilyard, A. C., Lagna, G., and Hata, A. (2008) *Nature* **454,** 51–61
56. Lee, Y., Kim, M., Han, J., Yeom, K. H., Lee, S., Baek, S. H., and Kim, V. N. (2004) *EMBO J.* **23,** 4051–4060
57. Si, M. L., Zhu, S., Wu, H., Lu, Z., Wu, F., and Mo, Y. Y. (2007) *Oncogene* **26,** 2799–2803
58. Asangani, I. A., Rasheed, S. A., Nikolova, D. A., Leupold, J. H., Colburn, N. H., Post, S., and Allgayer, H. (2008) *Oncogene* **27,** 2128–2136
59. Suzuki, H. I., Yamagata, K., Sugimoto, K., Iwamoto, T., Kato, S., and Miyazono, K. (2009) *Nature* **460,** 529–533
60. Peltier, H. J., and Latham, G. J. (2008) *RNA* **14,** 844–852
61. Kalomiris, E. L., and Bourguignon, L. Y. (1989) *J. Biol. Chem.* **264,** 8113–8119
62. Bourguignon, L. Y., Lokeshwar, V. B., He, J., Chen, X., and Bourguignon, G. J. (1992) *Mol. Cell. Biol.* **12,** 4464–4471
63. Legg, J. W., Lewis, C. A., Parsons, M., Ng, T., and Isacke, C. M. (2002) *Nat. Cell Biol.* **4,** 399–407
64. Fanning, A., Volkov, Y., Freeley, M., Kelleher, D., and Long, A. (2005) *Int. Immunol.* **17,** 449–458
65. Mackay, H. J., and Twelves, C. J. (2003) *Endocr. Relat. Cancer* **10,** 389–996
66. Kuroda, T., Tada, M., Kubota, H., Kimura, H., Hatano, S. Y., Suemori, H., Nakatsuji, N., and Tada, T. (2005) *Mol. Cell Biol.* **25,** 2475–2485
67. Rodda, D. J., Chew, J. L., Lim, L. H., Loh, Y. H., Wang, B., Ng, H. H., and Robson, P. (2005) *J. Biol. Chem.* **280,** 24731–24737
68. Do, J. T., and Schöler, H. R. (2006) *Ernst Schering Res. Found. Workshop* **60,** 35–45
69. Chan, J. A., Krichevsky, A. M., and Kosik, K. S. (2005) *Cancer Res.* **65,** 6029–6033
70. Cheng, A. M., Byrom, M. W., Shelton, J., and Ford, L. P. (2005) *Nucleic Acids Res.* **33,** 1290–1297
71. Yang, H. S., Jansen, A. P., Komar, A. A., Zheng, X., Merrick, W. C., Costes, S., Lockett, S. J., Sonenberg, N., and Colburn, N. H. (2003) *Mol. Cell Biol.* **23,** 26–37
72. Suzuki, C., Garces, R. G., Edmonds, K. A., Hiller, S., Hyberts, S. G., Marintchev, A., and Wagner, G. (2008) *Proc. Natl. Acad. Sci. U.S.A.* **105,** 3274–3279
73. Loh, P. G., Yang, H. S., Walsh, M. A., Wang, Q., Wang, X., Cheng, Z., Liu, D., and Song, H. (2009) *EMBO J.* **28,** 274–285
74. Hunter, A. M., LaCasse, E. C., and Korneluk, R. G. (2007) *Apoptosis* **12,** 1543–1568
75. Hanahan, D., and Weinberg, R. A. (2000) *Cell* **100,** 57–70
76. Evan, G. I., and Vousden, K. H. (2001) *Nature* **411,** 342–348
77. LaCasse, E. C., Baird, S., Korneluk, R. G., and MacKenzie, A. E. (1998) *Oncogene* **17,** 3247–3259
78. Juliano, R. L., and Ling, V. A. (1976) *Biochim. Biophys. Acta* **455,** 152–162
79. Gros, P., Croop, J., and Housman, D. (1986) *Cell* **47,** 371–380
80. Higgins, C. F. (1992) *Annu. Rev. Cell Biol.* **8,** 67–113
81. Fojo, A. T., Ueda, K., Slamon, D. J., Poplack, D. G., Gottesman, M. M., and Pastan, I. (1987) *Proc. Natl. Acad. Sci. U.S.A.* **84,** 265–269

82. Wickramasinghe, N. S., Manavalan, T. T., Dougherty, S. M., Riggs, K. A., Li, Y., and Klinge, C. M. (2009) *Nucleic Acids Res.* **37,** 2584–2595
83. Miletti-González, K. E., Chen, S., Muthukumaran, N., Saglimbeni, G. N., Wu, X., Yang, J., Apolito, K., Shih, W. J., Hait, W. N., and Rodríguez-Rodríguez, L. (2005) *Cancer Res.* **65,** 6660–6667
84. Chambers, I., Colby, D., Robertson, M., Nichols, J., Lee, S., Tweedie, S., and Smith, A. (2003) *Cell* **113,** 643–655
85. Mitsui, K., Tokuzawa, Y., Itoh, H., Segawa, K., Murakami, M., Takahashi, K., Maruyama, M., Maeda, M., and Yamanaka, S. (2003) *Cell* **113,** 631–642
86. Ezeh, U. I., Turek, P. J., Reijo, R. A., and Clark, A. T. (2005) *Cancer* **104,** 2255–2265
87. Zhang, J., Wang, X., Li, M., Han, J., Chen, B., Wang, B., and Dai, J. (2006) *FEBS J.* **273,** 1723–1730
88. Lu, D., Sivaprasad, U., Huang, J., Shankar, E., Morrow, S., and Basu, A. (2007) *Apoptosis* **12,** 1893–1900
89. Lu, Z., Liu, M., Stribinskis, V., Klinge, C. M., Ramos, K. S., Colburn, N. H., and Li, Y. (2008) *Oncogene* **27,** 4373–4379
90. Frankel, L. B., Christoffersen, N. R., Jacobsen, A., Lindow, M., Krogh, A., and Lund, A. H. (2008) *J. Biol. Chem.* **283,** 1026–1033
91. Meng, F., Henson, R., Wehbe-Janek, H., Ghoshal, K., Jacob, S. T., and Patel, T. (2007) *Gastroenterology* **133,** 647–658